

# MODELLING HEAT TRANSFER IN AN EXTRUDER FOR RECYCLING PLASTICS INTO FILAMENTS FOR USE IN ADDITIVE MANUFACTURING

Meysam Nasr Azadani<sup>a</sup>, Esther Akinlabi<sup>b</sup>, Timothy Whitehead<sup>c</sup>, Muyiwa Oyinlola<sup>a\*</sup>

\*Author for correspondence

<sup>a</sup>Institute of Energy and Sustainable Development,  
De Montfort University, Leicester UK, LE1 9BH

<sup>b</sup>Institute of Life and Earth Sciences, Pan African University, Ibadan Nigeria

<sup>c</sup>School of Engineering and Physical Science, Aston University, Birmingham, UK B4 7ET

E-mail: [muyiwa.oyinlola@dmu.ac.uk](mailto:muyiwa.oyinlola@dmu.ac.uk)

## ABSTRACT

Global production of plastic increased by 500% over the last 30 years and it is expected to continue to grow to 850 million tons/year by 2050. Plastic use results in a substantial environmental burden due to both land and water pollution as plastics take 10 to 450 years to decompose in landfills. This has resulted in increased calls for innovative ways to recycle plastics, one of which is a decentralised solution where wasted plastics are recycled into filaments for 3D printing. This has been identified as a promising solution, especially for low-income communities in the global south where waste management infrastructure is inadequate. However, studies have highlighted the need for more research and development in the extruder design and operation, especially in terms of optimising temperature distribution and the cooling rate in order to prevent poor filament quality and inconsistent filament diameter. This paper describes the modelling of the temperature distribution and cooling rate of an extruder. The innovation is that the extruder is designed to be built and operated in low-income settings of the global south using locally available materials and skills. The aim of the work is to develop a mathematical model for evaluating the thermal distribution in the extruder as well as optimise the cooling rate conditions. The model is useful for optimising the operating conditions such as ambient temperature, extrusion temperature, extrusion speed, cooling rate and spooling mechanism.

## INTRODUCTION

Environmental and consumer concerns has necessitated research into sustainable management of plastic materials. Plastic recycling has recently emerged as a critical problem in environmental preservation and waste management. Due to the low cost, lightweight, and superior protection they offer, plastic is frequently the material of choice for the packaging of food, cosmetics, or pharmaceutical items [1]. However, improper disposal of plastics at end of life has resulted in an environmental burden due to both land and water pollution as plastics take 10 to 450 years to decompose in landfills. One way of reducing the environmental footprint of plastics is by adopting a decentralised recycling approach where waste plastics are extruded into filaments for Additive Manufacturing (3D Printing). Petrochemical plastics, in general, offer great functionality for use as filaments for 3D printing, therefore waste plastics offer an opportunity to cater for the rapidly expanding 3D printing

market and allows for successful waste use to create consumable goods.

## NOMENCLATURE

|            |                        |  |
|------------|------------------------|--|
| $\rho$     | [kg/m <sup>3</sup> ]   | Density                                |
| $c$        | [W·s/kg·°C]            | Specific heat                          |
| $q$        | [W/m <sup>2</sup> ]    | Heat flux                              |
| $A$        | [m <sup>2</sup> ]      | Area                                   |
| $l$        | [m]                    | Length                                 |
| $r$        | [m]                    | Radius                                 |
| $k$        | [W/m°C]                | Thermal conductivity                   |
| $T$        | [°C]                   | Temperature                            |
| $x$        | [m]                    | Cartesian axis direction               |
| $y$        | [m]                    | Cartesian axis direction               |
| $z$        | [m]                    | Cartesian axis direction               |
| $C1$       | -                      | Constant                               |
| $C2$       | -                      | Constant                               |
| $\theta$   | -                      | Spatial temperature distribution       |
| $T_i$      | [°C]                   | Initial temperature                    |
| $T_\infty$ | [°C]                   | Ambient temperature                    |
| $\bar{h}$  | [W/m <sup>2</sup> ·°C] | Heat transfer coefficient              |
| $\tau(t)$  |                        | Function of the time only              |
| $R(r)$     |                        | Function of the radial coordinate only |
| $X(x)$     |                        | Function of the x coordinate only      |
| $J_0$      | -                      | First Bessel function                  |
| $J_1$      | -                      | Second Bessel function                 |
| $C_{nm}$   | -                      | Constant                               |
| $C_n$      | -                      | Constant                               |
| $C_m$      | -                      | Constant                               |
| $\lambda$  | -                      | Eigenvalue                             |
| $F_o$      | -                      | Fourier Number                         |
| $Bi$       | -                      | Biot Number                            |
| $Bi_x$     |                        | Biot number in the x-direction         |
| $Bi_r$     |                        | Biot number in the r-direction         |
| $\alpha$   | [m <sup>2</sup> /s]    | Thermal diffusivity                    |
| $PET$      | -                      | Polyethylene terephthalate             |
| $ABS$      | -                      | Acrylonitrile-Butadiene-Styrene        |
| $AM$       | -                      | Additive Manufacturing                 |

Plastic extrusion is one of the most used production procedures for creating polymers, and it is especially common for thermoplastics. Green composite filaments derived from recycled cellulose and rubber-based materials can result in 3D-printed products with increased stiffness, durability, and/or

decreased distortion [2]. Because of the poor value of recovered content and high transportation and collecting expenses, plastic recycling is currently limited. However, distributed production via additive manufacturing (AM), in which 3D printing filament is manufactured from local plastic waste, is an economically feasible alternative to plastic recycling [3].

During the extrusion process, solid polymer particles are heated to the melting point in the early stage of the extruder. The liquid polymer is heated to a temperature much over the melting point in the middle of the extruder, while the solid particles continue to heat up and melt. The molten polymer must attain a thermally homogenous condition in the last section of the extruder. When the extrudate exits the extruder die, it must be cooled to room temperature. Every extruded shape must be cooled to the point where it retains its specified dimensions. Temperature conditions are critical for minimising warpage. If the extrudate is pulled across a sharp surface as it exits the die, enters the cooling fixture, or at any other site, warpage occurs in the component. Figure 1 shows the effect of colling on the quality of extruded products.

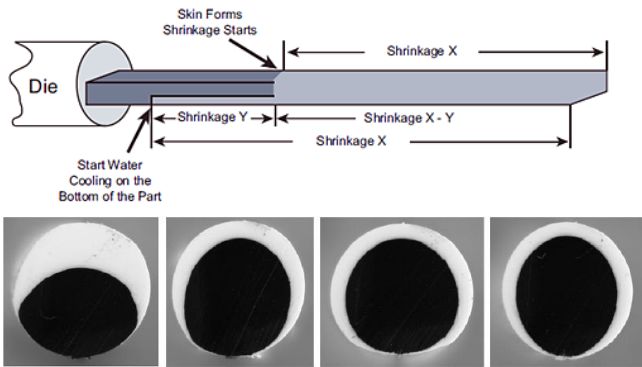


**Figure 1** Effect of cooling on shrinkage and deformation of extruded product through a circular channel [4]

It is important to note that the rate of cooling has a huge effect on the quality of the product. High-molecular orientation in one location of the extrudate induces distinct shrinkage in other places, resulting in warpage [5]. Process cooling is a typical procedure in extrusion to keep the process thermally stable. In addition, as part of the process heat is naturally emitted into the environment. As a result, the cooling water and air absorb a significant percentage of the energy given to the process. In reality, it is evident that a significant portion of the given energy must be sacrificed in order to preserve the process's thermal stability. Obviously, process energy and thermal efficiency are likely to be linked. Making the process more energy-efficient, however, is pointless if the melt output is not of the desired quality. As a result, thermal stability and energy efficiency should be pursued in a sequential manner.

Similarly, the homogeneity of the melted plastic being fed into the die, which should preferably be provided at a consistent pressure, temperature, and circulation, is critical to the quality of extruded polymer. Thermal stability is critical in polymer

extrusion because the amount of melt homogeneity attained by the extruder screw determines product quality. Figure 2 shows the temperature distribution in an extrusion process. It can be observed that the polymer goes through a convoluted temperature history over this entire operation. Therefore, a detailed understanding of the heat transfer process is necessary to optimize design and operating parameters of the extrusion process. This paper describes the modelling of the temperature distribution and cooling rate of an extruder. The model is useful for optimising the operating conditions such as ambient temperature, extrusion temperature, extrusion speed, cooling rate and spooling mechanism.

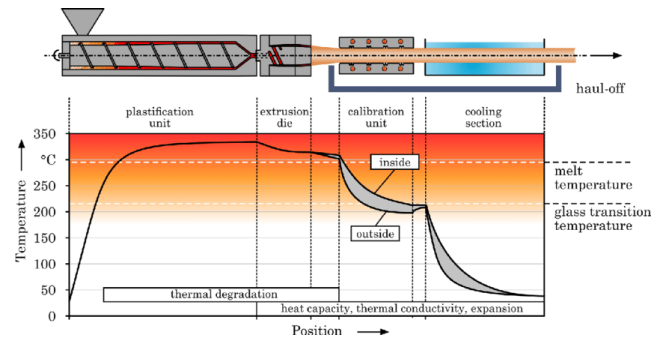


**Figure 2** Temperature distribution in a whole extrusion process [6]

## PET

PET, which stands for polyethylene terephthalate, is a transparent, durable, and lightweight polyester plastic. When used for fibres or textiles, it is commonly referred to as "polyester," and when used for bottles, jars, containers, and packaging purposes, it is referred to as "PET" or "PET Resin." PET was originally polymerized by DuPont researchers in the 1940s [7] to produce thermoplastics for use as textile materials. It is created by combining ethylene glycol with terephthalic acid. PET is exceptionally robust for its light weight even without additives to boost its robustness.

PET is widely used for diverse applications across various sectors, it makes up a substantial proportion of the plastic waste stream [8]. This, coupled with the fact that it is not biodegradable, makes reusing or recycling a practical way to reduce PET waste [9]. Moreover, in 2030, the global demand for PET is forecasted to amount to 42 metric tons [10]. Therefore, the viability of filaments from recycled materials in low-income economies depends heavily on successfully converting PET waste to filaments.

PET is an excellent material for 3D printing [11] as it is a robust and flexible material with a high success rate. It is ideal for products that require both flexibility and hardness, like mechanical components or electrical equipment enclosures. PET is known for releasing less odour than standard 3D printing materials such as ABS [12].

The filament is ideal for companies looking to make their distribution network more sustainable, especially when

combined with 3D printing technology for manufacturing output. The carbon footprint of recycled filament is smaller than that of virgin material and PET is not excepted

Table 1 indicates several characteristics of a few polymers including PET.

**Table 1** Properties of polymers [13]

| Polymer  | Solid density | Melt density | Melting point C | Heat capacity | Thermal conductivity |
|----------|---------------|--------------|-----------------|---------------|----------------------|
| PET      | 1.34-1.39     | 1160         | 265             | 1800-2000     | 0.18                 |
| ABS      | 1.01-1.04     | 990          | Amorphous*      | 1300-1700     | 0.25                 |
| Nylon-66 | 1.13-1.15     | 980          | 265             | 2400-2600     | 0.2                  |

## MATHEMATIC MODELLING

The general mathematical formula that governs the unsteady-conduction of heat across a two-dimensional solid in cylindrical coordinates is given in equation (1), where heat transfer is assumed to be significant in the radial ( $r$ ) and longitudinal ( $x$ ) directions but completely disregarded in the angular direction due to symmetry boundary conditions, and the thermo-physical parameters  $\rho$ ,  $c$ , and  $k$  are assumed to be constant for simplicity. According to Newton's law of cooling, the filament may lose heat from its outside surface. Because the condition is symmetrical in axial position  $x$ , only half of the extruded filament's length is taken into account. The heat transfer equation is a partial differential equation that represents the temperature distribution in a given region over time as follows [14],[15]:

$$\rho c \frac{dy}{dx} = -div q + \dot{w} \quad (1)$$

For 2D solid cylindrical coordinates

$$\frac{1}{r} \frac{\partial}{\partial r} \left( r \frac{\partial T}{\partial r} \right) + \frac{\partial^2 T}{\partial x^2} + q = \frac{1}{\alpha} \frac{\partial T}{\partial t}$$

To keep the boundary conditions uniform, first defined as the spatial temperature profile with respect to the given ambient temperature  $T$ . Moreover, the starting temperature is specified as  $\theta_i = T_{initial} - T_{ambient}$ . As a result, the initial condition and the boundary requirements that must be met are as follows:

$$\begin{aligned} \text{BC 1} \quad & \frac{\partial \theta(r, x, t)}{\partial r} = 0 \rightarrow r = 0, x, t \rightarrow, \frac{\partial \theta(0, x, t)}{\partial r} = 0 \\ \text{BC 2} \quad & \frac{\partial \theta(r, x, t)}{\partial r} = 0 \rightarrow r = a, x, t \rightarrow \frac{\partial \theta(r, x, t)}{\partial r} = -\frac{h}{k} \theta(a, x, t) \\ \text{BC 3} \quad & \frac{\partial \theta(r, x, t)}{\partial x} = 0 \rightarrow r, x = 0, t \rightarrow, \frac{\partial \theta(0, 0, t)}{\partial x} = 0 \\ \text{BC 4} \quad & \frac{\partial \theta(r, x, t)}{\partial x} = 0 \rightarrow r, x = l, t \rightarrow, \frac{\partial \theta(r, x, t)}{\partial x} = -\frac{h}{k} \theta(r, l, t) \end{aligned}$$

As a result of all of these considerations, a solution that is the product of three functions in the form of variable separation has been available, specifically,  $R(r)$  is a function of the radial coordinate only,  $X(x)$  is a function of the  $x$  coordinate alone, and  $\tau(t)$  is a function of the time only. As a result of using this solution, the overall solution is expressed as

$$\theta(r, x, t) = R(r) \cdot X(x) \cdot \tau(t) \quad (2)$$

This equation is substituted for into partial differential equation (1), yielding the following conclusion.

$$X(x) \cdot \tau(t) \cdot \frac{1}{r} \frac{\partial}{\partial r} \left( r \frac{\partial T}{\partial r} \right) + R(r) \cdot \tau(t) \cdot \frac{\partial^2 X(x)}{\partial x^2} = \frac{R(r) \cdot X(x) \cdot \tau(t)}{\alpha} \cdot \frac{\partial \tau(t)}{\partial t} \quad (3)$$

Equation (3) is therefore divided by the product  $R(r)Z(z)(t)$  solution, yielding:

$$\frac{\ddot{R}}{R} + \frac{1}{r} \frac{\dot{R}}{R} + \frac{\ddot{X}}{X} = \frac{1}{\alpha} \frac{\dot{\tau}}{\tau} \quad (4)$$

The separation constant is adjusted so that the left and right-hand side terms are equal to  $-\alpha^2$  and  $-\beta^2$ , respectively, and the right-hand side term is equal to  $-(\alpha^2 + \beta^2)$ . These give rise to three ordinary differential equations, which may be solved using the equations presented below.

$$\begin{aligned} \frac{\ddot{R}}{R} + \frac{1}{r} \frac{\dot{R}}{R} &= -\alpha^2 \\ \frac{\ddot{X}}{X} &= -\beta^2 \\ \frac{1}{\alpha} \frac{\dot{\tau}}{\tau} &= -(\alpha^2 + \beta^2) \end{aligned} \quad (5)$$

These ordinary differential equations, when combined with their boundary conditions stated as first-order equations, yield the solutions shown below. The answer for  $R$  in the  $r$  model is as follows:

$$r^2 \ddot{R} + r \dot{R} + \alpha^2 r^2 R = 0 \quad (6)$$

$$R(r) = C_1 J_0(\alpha r) + C_2 Y_0(\alpha r)$$

Where  $J_0$  and  $Y_0$  are recognized zero-order Bessel functions of the first and second class. In this formula, coefficient  $C_2$  is deleted by applying b.c. (1), because all  $Y_n$  become - as  $r$  approaches zero; hence,  $C_2 = 0$  is necessary to maintain the finite solution. Using the convection b.c. (2) formulae for the derivative of  $J_0$  as  $dJ_0(r)dr = -J_1(r)$ , the relevant eigenvalue connection is obtained. This is the eigencondition for that issue, and which may be expressed as:

The Biot number in the direction of  $r$  is equivalent to  $hr/k$ , and  $Bi_r$  is the Biot number in the direction of  $r$ . Furthermore, the eigenvalues are given by the roots of equation (6), and there exist an unlimited number of real eigenvalues such as  $a_1r, a_2r, a_3r, \dots, anr$ . And, as shown in the figure, all of these values may be represented visually as intersections of the graph of  $J_0(\lambda) / J_1(\lambda)$  with the graph of a straight line through the origin with a slope of  $\lambda / Bi_r$ . The general result of the second term of equation (2) in the  $x$ -direction, on the other hand, is stated as:

$$\ddot{X} + \beta^2 X(x) = 0 \quad (7)$$

$$X(x) = C_3 \sin(\beta x) + C_4 \cos(\beta x)$$

The coefficient  $C_3$  in this equation is readily removed by using b.c.(3) in order to meet the criterion, namely,  $C_3$  must be

equivalent to 0. Then, using convection b.c (4), the following required eigenvalue relationship is established:

$$-\beta C_4 \sin(\beta l) = -\frac{h}{k} C_4 \cos(\beta l) \quad (8)$$

This is another eigencondition required for this issue and can be represented as the following formula to produce a boolean equation for  $\beta$ .

$$\tan(\beta c) = \frac{Bi_x}{\beta l}, \quad Bi_x = \frac{hl}{k} \quad (9)$$

where  $Bi_x$  is the Biot number in the x-direction equal to  $hl/k$ . In this case, the infinite roots that fulfil the equation (9) are  $\beta 1_x, \beta 2_x, \beta 3_x, \dots, \beta m_x$ , where  $\beta m < \beta m+1$ , ( $m = 1, 2, \dots$ ); and the acceptable values of these positive roots are indicated as the intersections of the graph of the  $\cot(\lambda)$  with the graph of a straight line through the origin with a slope of  $\beta m_x / Bi_x$ .

The values of  $\lambda_m$ , in this case, like the preceding eigenvalues for  $J_0$ , are not uniformly distributed and must be determined numerically. As the integer  $m$  grows, so do these values of  $\lambda_m$ , and as a result, the intersections become closer to a numerical value of  $\pi$  while the cotangent term grows to infinity. Consequently, the general solution of the third in the t equation is found as:

$$\begin{aligned} \dot{\tau}(t) + (\alpha_n^2 + \beta_n^2) a \tau(t) &= 0 \\ \tau(t) &= e^{-(\alpha_n^2 + \beta_n^2) at} \end{aligned} \quad (10)$$

Because there are an infinite number of references for both  $n$  and  $m$ , the answer is a double summation of all  $n$ 's and  $m$ 's. As a result, the product solution for  $\theta(r,z,t) = R(r)Z(z)T(t)$  is written as follows:

$$\theta(r, x, t) = \sum_{n=1}^{\infty} \sum_{m=1}^{\infty} C_{nm} J_0(\alpha r) * \cos(\beta x) * e^{-(\alpha_n^2 + \beta_n^2) at} \quad (11)$$

There are an unlimited number of roots in  $r$  and  $x$ , thus the initial condition  $\theta_i$  is applied and it is supposed that is equivalent to a sequence of equations with unknown  $C_{nm}$ .

$$\theta_i = \sum_{n=1}^{\infty} \sum_{m=1}^{\infty} C_{nm} J_0(\alpha r) * \cos(\beta x) \quad (12)$$

The orthogonality features of Bessel functions and  $\cos$  functions with regard to the weighting factor  $r$  across the finite interval  $0, x$ , and  $0, l$  are used to solve the following problem. It is obtained by multiplying both sides of the equation by  $J(\alpha_n r) * r$  and  $\cos(\beta m x)$ , then integrating the result throughout the interval using the assumption that the integral of the infinite sum is the sum of integrals. As a result, formula (12) may be simplified as:

$$\begin{aligned} \int_0^a \theta_i r J_0(\alpha_n r) dr \int_0^c \cos(\beta_m x) & \\ = C_{nm} \int_0^a r J_0^2(\alpha_n r) dr \int_0^c \cos^2(\beta_m x) & \end{aligned} \quad (13)$$

Calculating the integrals for  $\theta_i$  which is equivalent to:

$$\begin{aligned} \theta &= T_i - T_{\infty} \\ \theta_i &= \frac{a}{\alpha_n} J_1(\alpha_n a) \frac{\sin(\beta_m x)}{\beta_m} \\ &= C_{nm} \frac{a^2}{2} [J_1^2(\alpha_n a) + J_0^2(\alpha_n a)] * \left[ \frac{l}{2} \right. \\ &\quad \left. + \frac{\cos(\beta_m l)}{2\beta_m} \sin(\beta_m l) \right] \end{aligned} \quad (14)$$

By simplifying the preceding formula, we get:

$$\begin{aligned} C_{nm} &= \theta_i C_n C_m \\ C_{nm} &= \theta_i \frac{2a J_1(\alpha_n a)}{\alpha_n a^2 [J_1^2(\alpha_n a) + J_0^2(\alpha_n a)]} * \frac{2 \sin(\beta_m l)}{\beta_m \left[ \frac{l}{2} + \frac{\cos(\beta_m l)}{2\beta_m} \sin(\beta_m l) \right]} \end{aligned} \quad (15)$$

As a result, expression (15) yields an equation for the constants:

$$C_n = \frac{2a J_1(\alpha_n a)}{\alpha_n a^2 [J_1^2(\alpha_n a) + J_0^2(\alpha_n a)]} = \frac{2 Bi_a}{(Bi^2 + \lambda_n^2) J_0(\lambda_n)} \quad (16)$$

$$C_m = \frac{2 \sin(\beta_m l)}{\beta_m \left[ \frac{l}{2} + \frac{\cos(\beta_m l)}{2\beta_m} \sin(\beta_m l) \right]} = \frac{2 \sin(\beta_m l)}{\beta_m l + \cos(\beta_m l) \sin(\beta_m l)} \quad (17)$$

The final answer in dimensionless form is achieved by substituting these parameters into equation (11):

$$\begin{aligned} \theta(r, x, t) &= 2 \theta_i Bi \sum_{n=1}^{\infty} \frac{J_0(\lambda_n \frac{r}{a}) e^{-\lambda_n^2 F_0}}{(Bi^2 + \lambda_n^2) J_0(\lambda_n)} \\ &\quad * 2 \sum_{m=1}^{\infty} \frac{\sin(\beta_m l) \cos(\beta x) e^{-\beta_m^2 at}}{\beta_m l + \sin(\beta_m l) \cos(\beta_m l)} \end{aligned} \quad (18)$$

Where;

$$F_0 = \frac{\alpha t}{l^2}, \quad \alpha_n l = \lambda_n, \quad Bi = \frac{hl}{k}, \quad l = \frac{V}{A} \quad (19)$$

## RESULTS

The representation of the analytical solutions is given in the following figures. By using the exact analytical solutions listed in this section and implemented in Matlab software, the 2D plot of temperature per unit length and time is derived.

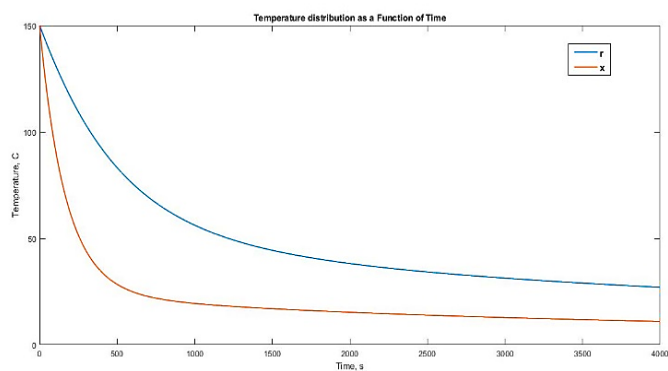


**Figure 3** Temperature distribution at r and x direction as a function of time

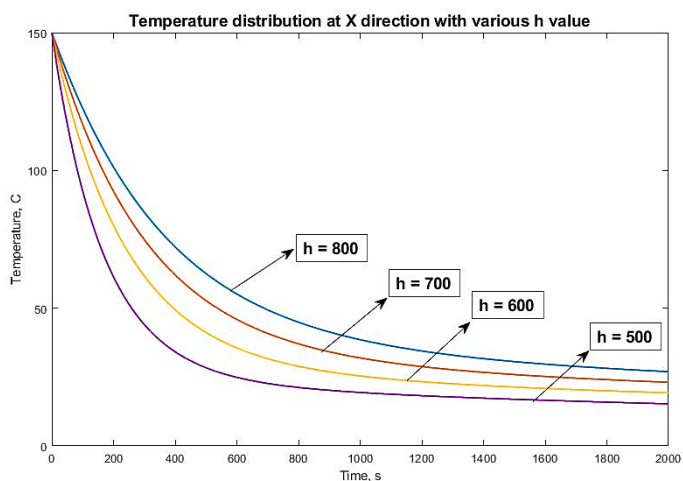


**Figure 4** Temperature distribution at x direction with different value of h coefficient

In detail, the temperature distribution of the analytical solution as a function of radial distance and time, and also as a function of longitudinal distance is shown in Figure 3, respectively. Obviously, the filament is cooled suddenly in both directions. The rate of cooling for the filament is significantly decreased. The cooling rate in the  $x$  direction is less than that of the  $r$  direction takes more time to be cooled.

Figure 4 shows the temperature profile at different values of heat transfer coefficients, which represents varying operating conditions such as cooling of extrudate, speed of extrusion, cooling medium e.t.c. The profile is useful for adjusting various parameters such as extrusion speed, cooling rate and spooling mechanism.

## CONCLUSION

The art of reusing materials particularly waste plastics has been of interest to the researcher in order to manage the rate of waste materials with the help of additive manufacturing when it comes to the environment. PET as a kind of material used for additive manufacturing, can be a great choice. Considering the

good quality of the extruded filament, thermal stability and heat transfer of extrusion are of importance. In this research study, the role of heat transfer of filament extruded from die was investigated mathematically. Applying for the unsteady transient heat transfer, a circular extruded filament was numerically considered in the 2D direction. The numerical results represent the time-dependent temperature distribution of filament in radial and longitudinal directions. It was found that the cooling rate figures for both directions are somehow in the same state, but the rate of cooling in the  $Z$  direction happened sooner than in the  $r$  direction. The next research idea would be the heat transfer modelling of extruded filament considering all thermal stabilities of pre-die (extruder), die, and post-die sections to gain a favourable quality of extruded filament applicable for additive manufacturing.

## ACKNOWLEDGEMENT

This work is supported by the UKRI GCRF under Grant EP/T0238721 and the British Council Innovation for African University Circular Plastic Economy Innovation Hub Grant.

## REFERENCES

- [1] Coltelli, M.-B.; Gigante, V.; Cinelli, P.; Lazzeri, A. Chapter 15 Flexible Food Packaging Using Polymers from Biomass. In *Bionanotechnology to Save the Environment; Plant and Fishery's Biomass as Alternative to Petrol*; Morganti, P., Ed.; MDPI: Basel, Switzerland, 2018; pp. 272–296.
- [2] Zander, N., Park, J., Boelter, Z., & Gillan, M. (2019). Recycled Cellulose Polypropylene Composite Feedstocks for Material Extrusion Additive Manufacturing. *ACS Omega*, 4(9), 13879-13888. <https://doi.org/10.1021/acsomega.9b01564>
- [3] Nicole E. Zander Polymer-Based Additive Manufacturing: Recent Developments. January 1, 2019, 37-51, DOI:10.1021/bk-2019-1315.ch003
- [4] Chung, C. (2019). *Extrusion of Polymers 3E* (pp. 417-418). Cincinnati: Hanser Publications.
- [5] Vaes, D., & Van Puyvelde, P. (2021). Semi-crystalline feedstock for filament-based 3D printing of polymers. *Progress In Polymer Science*, 118, 101411. <https://doi.org/10.1016/j.progpolymsci.2021.101411>
- [6] Stegelmann, M., Müller, M., Winkler, A., Liebsch, A., & Modler, N. (2018). Polymer Analyses for an Adapted Process Design of the Pipe-Extrusion of Polyetherimide. *Materials Sciences and Applications*, 09, 614-624.
- [7] Ji, Li Na (June 2013). "Study on Preparation Process and Properties of Polyethylene Terephthalate (PET)". *Applied Mechanics and Materials*. 312: 406–410. Bibcode:2013AMM...312..406J. doi:10.4028/www.scientific.net/AMM.312.406. S2CID 110703061.
- [8] Adefila, A., Abuzeinab, A., Whitehead, T., & Oyinlola, M. (2020). Bottle house: utilising appreciative inquiry to develop a user acceptance model. *Built Environment Project and Asset Management*,
- [9] Zander, N. E., Gillan, M., & Lambeth, R. H. (2018). Recycled polyethylene terephthalate as a new FFF feedstock material. *Additive Manufacturing*, 21, 174-182.
- [10] Dybka-Stepień, K., Antolak, H., Kmiolek, M., Piechota, D., & Koziróg, A. (2021). Disposable Food Packaging and Serving Materials—Trends and Biodegradability. *Polymers*, 13(20), 3606.
- [11] Oussai, A., Bártfai, Z., & Kátai, L. (2021). Development of 3D Printing Raw Materials from Plastic Waste. A Case Study on Recycled Polyethylene Terephthalate. *Applied Sciences*, 11(16), 7338. <https://doi.org/10.3390/app11167338>

- [12] Mikula, K., Skrzypczak, D., Izydorczyk, G., Warchoń, J., Moustakas, K., Chojnacka, K., & Witek-Krowiak, A. (2020). 3D printing filament as a second life of waste plastics—a review. *Environmental Science And Pollution Research*, 28(10), 12321-12333. <https://doi.org/10.1007/s11356-020-10657-8>
- [13] Oussai, A., Bártfai, Z., & Kátai, L. (2021). Development of 3D Printing Raw Materials from Plastic Waste. A Case Study on Recycled Polyethylene Terephthalate. *Applied Sciences*, 11(16), 7338. <https://doi.org/10.3390/app11167338>
- [14] degli Studi di Cagliari. (2015). *Analytical solutions of the steady or unsteady heat conduction equation in industrial devices: A comparison with FEM results*. (PhD).
- [15] HAN, J. (2022). *ANALYTICAL HEAT TRANSFER*. CRC PRESS.